© Universiti Tun Hussein Onn Malaysia Publisher's Office

IJIE

Journal homepage: http://penerbit.uthm.edu.my/ojs/index.php/ijie

The International Journal of Integrated Engineering

Neural-Network Based Adaptive Proxemics-Costmap for Human-Aware Autonomous Robot Navigation

Chik Sheng Fei[1], Yeong Che Fai[2*], Eileen Su Lee Ming[1], Lim Thol Yong[3], Duan Feng[4], Patrick Chin Jun Hua[5]

[1]School of Electrical Engineering, Faculty of Engineering, Universiti Teknologi Malaysia, Johor Bahru, 81310, MALAYSIA

[2]Centre for Artificial Intelligence and Robotics, Faculty of Engineering, Universiti Teknologi Malaysia, Johor Bahru, 81310, MALAYSIA

[3]Malaysia Japan Institute of Technology (MJIIT), Universiti Teknologi Malaysia, Kuala Lumpur, 54100, MALAYSIA

[4]Department of Automation, College of Computer and Control Engineering, Nankai University, Tianjin, 300071, CHINA

[5]DF Automation and Robotics Sdn. Bhd, Johor Bahru, 81300, MALAYSIA

*Corresponding Author

DOI: https://doi.org/10.30880/ijie.2019.11.04.011
Received 25 April 2019; Accepted 31 July 2019; Available online 5 September 2019

Abstract: In the revolution of Industry 4.0, autonomous robot navigation plays a vital role in ensuring intelligent cooperation with human workers to increase manufacturing efficiency. Human prefers to maintain a proxemic distance with other subjects for safety and comfort purposes, where the human personal-space can be represented by a costmap. Current proxemic costmaps perform well in defining the proxemic boundary to maintain the human-robot proxemic distance. However, these approaches generate static costmaps that are not adaptive towards different human states (linear position, angular position and velocity). This problem impacts the robot navigation efficiency, reduces human safety and comfort as the autonomous robot failed to prioritize avoiding certain humans over the other. To overcome this drawback, this paper proposed a neural-network based adaptive proxemic-costmap, named as NNPC, that can generate different sized personal-spaces at different human state encounters. The proposed proxemic-costmap was developed by learning a neural-network model using real human state data. A total of three human scenarios were used for data collection. The data were collected by tracking the humans in video recordings. After the model was trained, the proposed NNPC costmap was evaluated against two other state-of-art proxemic costmaps in five simulated human scenarios with various human states. Results show that NNPC outperformed the compared costmaps by ensuring human-aware robot manoeuvres that have higher robot efficiency and increased human safety and comfort.

Keywords: Neural-network, proxemics, adaptive, costmap, human-aware

1. Introduction

Over the years, with the emergence of robots into the manufacturing industry, the manufacturing efficiency have increased. The continuous advancement of robot technologies in the field of navigation including localization, path planning, costmap design, obstacle sensing and tracking have drove revolutions to the industry. In the recent effort of transforming the industry towards Industry 4.0 [1], robot navigation remains a crucial part for a robot to co-exist with human co-workers. Humans prefer to maintain a certain proxemic distance [2] between themselves and robots for safety

*Corresponding author: cfyeong@fke.utm.my

and comfortability purposes. Humans are governed by invisible social rules, and these affect their movement during Human-Robot-Interaction (HRI). Hall [2] separates human personal-space into intimate, personal, social and public. Human personal-space are governed by complex rules, and it is vital for robot designers to ensure their robots abide to these rules to gain acceptance from human.

In the context of human-aware robot navigation, the human personal-space is represented by a costmap with high cost cells surrounding a human. Human-aware robot navigation is distinct from conventional navigation as it considers human safety, comfortability and path smoothness in the search of an optimum robot path without trading off navigation efficiency. There are various human-aware navigation methods [3]. This research focuses on improving the costmap method, where an adaptive Neural-Network based Proxemic Costmap (NNPC) is proposed. The rest of the article is organized as follows: Section 2 presents the literatures related to human-aware costmaps, Section 3 introduces the methods used to design, develop and evaluate NNPC, the result of NNPC performance evaluation is discussed in Section 4, and this article is concluded in Section 5.

2. Literature Review

Human-aware costmaps typically use self-defined or learnt proxemic model to generate human personal-space boundaries to prevent a robot from traversing too close to a human or human group. Papadakis et al. [4] proposed a costmap that represents different types of human social-zone using velocity and orientation dependent proxemic model. Gómez et al. [5] designed a costmap that uses various Gaussian models to generate personal-spaces for individuals and human-groups. Vega-Magro et al. [6] group individuals into human-group based on their relative distances and define a boundary surrounding the group to avoid a robot from interrupting the group formation. These prior mentioned methods excel in categorizing humans into different human groups and assign personal-space to respective formations. This prevents a robot from interrupting the human group activities. However, the methods are designed in static human contexts where when moving humans are encountered, a robot can still fail to maintain an appropriate human-robot proxemic distance.

Some researches focus solely on the costmap generation for the personal-space of an individual. Kirby et al. [7] used 2 Gaussian functions to represent the front and rear sides of a personal-space. They also utilized a pass-on-the-right proxemic model [8] to ensure a robot to always pass-by a human on a socially preferable side. Scandolo and Fraichard [9] designed a costmap that has a proxemic model dependent on the Hall's proxemic model [2], human motion and interaction between humans and other objects in an environment. Patompak et al. [10] introduced Social Relationship Model (SRM), an extended version of Social-Force Model (SFM) [11] to assign different sized personal-space to humans in an environment, based on the human position, velocity and social relationship. These proxemic costmaps only define the personal-space boundary for individuals, which can cause a robot to interrupt a group personal-space. Besides, their limited capability on human trajectory prediction can also cause poor navigation performance when a moving human or human group is encountered.

There are some approaches involve human path prediction capability to reason about human future movements. By assuming linear human motions, Kollmitz et al. [12] utilized a multi-layered costmap that populates human predicted trajectories using Gaussian functions with linear decaying amplitudes from the current human position. Karageorgas [13] reasons about human future paths using the Bayesian Human Motion Intentionality Prediction (BHMIP) [14], and represented the paths using a series of Gaussian function. These costmaps serve the purpose of maintaining a human-robot proxemic distance and to allow early preparation for collision avoidance.

In overall, the main drawback of these current proxemic costmap approaches are not adaptive towards different human states (linear position, angular position and velocity). In simple, same sized personal-spaces are generated even though the humans are located far or near a robot, moving towards or away a robot and moving fast or slow relative to a robot. Although certain costmaps [4, 7, 10] took consideration of human states, but those approaches are designed for less complex scenarios like static individuals and small human group encounters. This drawback causes a robot to not able to prioritize avoiding certain human over the other, which impacts the human-aware navigation performance in terms of human comfortability and navigation efficiency and even potentially causes safety issues such as increase in human-robot collisions. Hence, this research proposed the NNPC, an adaptive costmap that can adapt to different human states to overcome the drawback of current approaches. NNPC utilizes a learnt neural-network model to generate appropriately sized personal-space for encountered humans at different states. The neural-network model was trained using real human motion data.

3. Methodology

NNPC is designed using 3 main parts. The first part is the basic Gaussian function (f_{proxPL}) proposed by Kirby et al. [7] that forms the personal-space boundary of a human. The second part of NNPC is the human intention predictor (HI) presented by Karageorgas [13] used to predict human future trajectory and the third part, the main contribution of this research, is the neural-network proxemic model (f_{NN}) used to change the size of the personal-space in order to adapt to different human states.

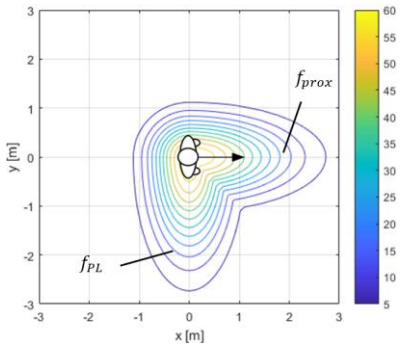

Fig. 1 – human personal-space costmap generated by f_{proxPL}.

The first part, f_{proxPL} (Fig. 1) is used in the design of NNPC because it provides a smooth exponential increasing cost from the personal-space boundary towards the center of a human position, thus allowing smooth robot paths to be planned in avoiding a human. f_{proxPL} can further be broken down into 2 minor parts. The first minor part is the proxemic function as follows:

$$f_{prox} = A exp\big(-(F_1 + F_2)\big) \tag{1}$$

where

$$F_1 = \frac{\left(\cos(\phi - \theta)\sqrt{(x_c - x_0)^2 + (y_c - y_0)^2}\right)^2}{2\sigma_x^2} \tag{2}$$

$$F_2 = \frac{\left(\sin(\phi - \theta)\sqrt{(x_c - x_0)^2 + (y_c - y_0)^2}\right)^2}{2\sigma_y^2} \tag{3}$$

$$\phi = \text{atan}\left(\frac{y_c - y_0}{x_c - x_0}\right) \tag{4}$$

$$\sigma_x = \begin{cases} \sigma_y^2(1 + \gamma v), & if\ |\phi - \theta| < 90° \\ \sigma_y^2, & otherwise \end{cases} \tag{5}$$

and A is the amplitude, σ_x^2 and σ_y^2 are the variances, γ is the velocity dependent factor and $|\phi - \theta|$ is the absolute value of the shortest angular difference. The second minor part is the passing layer, f_{PL}. f_{PL} is included in the design of NNPC to ensure the robot pass-by a human on a socially acceptable side. f_{PL} has the same equation as f_{prox} except for θ in Equation 2, 3 and 5 is changed to φ with the following equation:

$$\varphi = \begin{cases} \theta + 90°, & if\ pass\ on\ the\ right \\ \theta - 90°, & otherwise \end{cases} \tag{6}$$

Combining f_{prox} and f_{PL} (Equation 7) results in the first part of NNPC (f_{proxPL}) that generates a human personal-space boundary shown in Fig. 1.

$$f_{proxPL} = \max\{f_{prox}, f_{PL}\} \tag{7}$$

The second part of NNPC is HI. HI is vital in the design of NNPC as it predicts the human future trajectory for a robot to have early preparation for collision avoidance. HI computes the most probable human destination using Hidden Markov Models (HMM) [15] where Karageorgas [13] provided a detail explanation on the algorithm. Then, using A* [16] algorithm, a shortest path is planned from the human current position towards the most probably destination to represent the predicted human trajectory. The human trajectory is then populated with a series of Gaussian function (f_{proxPL}) using the following equation:

$$f_{proxHIPL} = \max\{f_{proxPL_1}, f_{proxPL_2} \cdots f_{proxPL_N}\} \tag{8}$$

where

$$N = \frac{relative\_distance}{v_q \times f} \tag{9}$$

and N is the total number of populated personal-space, which is influenced by the human-robot relative distance, robot's velocity, v_q and the velocity dependent factor, f. Fig. 2 shows the costmap generated by $f_{proxHIPL}$.

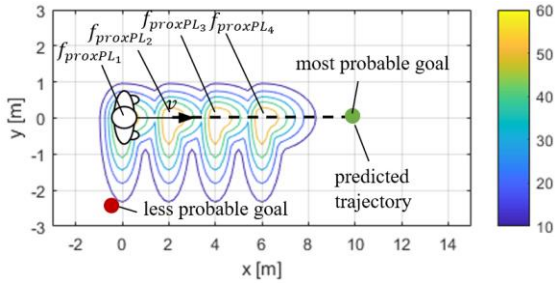

Fig. 2 – human personal-space costmap generated by $f_{proxHIPL}$.

The third part of NNPC is f_{NN}, the neural-network proxemic model. f_{NN} is designed to take in 3 input human states which relates to angular position, velocity and linear position, and have an output as a weight to control the size of the personal-space generated by $f_{proxHIPL}$. These inputs are selected based on several costmap approaches [4, 7, 10]. NNPC has the following equation:

$$f_{NNPC} = f_{NN} \times f_{proxHIPL} \tag{10}$$

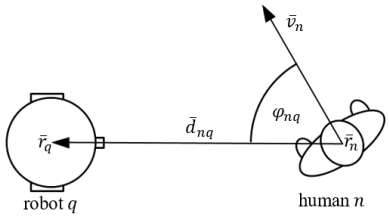

Fig. 3 – robot q encounters human n.

In the context of robot q and human n as shown in Fig. 3, (let n be the general notation to represent any human), the first input is the angular position, which is represented by anisotropic factor, $\omega(\varphi_{nq})$ [17]. The second input is the normalized human-robot relative velocity ($\tilde{v}_{nq}$) while the third input is the normalized human-robot relative distance ($\tilde{d}_{nq}$), both are normalized to the range of 0 to 1 using the min max normalization [18] method. f_{NN} is a feedforward multilayer perceptrons neural-network model as shown in Fig. 4.

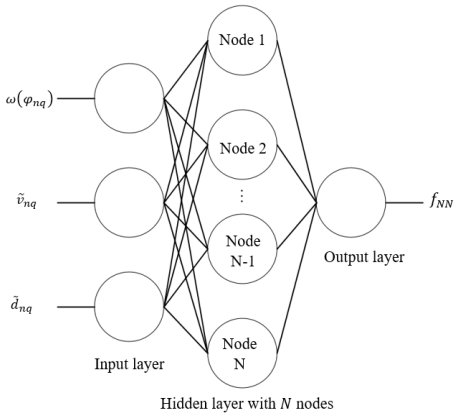

Fig. 4 – f_{nn} of NNPC with N nodes in the hidden layer.

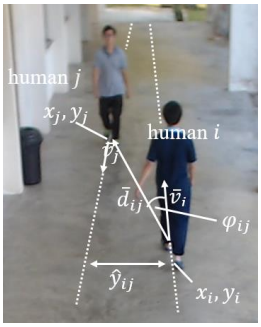

Fig. 4 – human i encounters human j.

As mentioned earlier, NNPC was designed where f_{NN} was trained using real human state data, as in several human-aware navigation literatures [19-22] suggested human is an appropriate demonstrator to teach a robot to react in a human environment. The human movements were recorded using video recording method and the human state data were collected by tracking the human movements in the footages. The input data and the training data have the same formula, but the latter relate to the states of humans i and j as shown in Fig. 5 instead of human n and robot q. The first training data is $\omega(\varphi_{ij})$, the anisotropic factor, the second training data is the normalized relative velocity ($\tilde{v}_{ij}$) and the third training data is the normalized relative distance ($\tilde{d}_{ij}$). The target data is the lateral distance between humans i and j ($\tilde{y}_{ij}$). $\tilde{y}_{ij}$ is chosen as the target data as it represented the proxemic distance humans prefer to maintain during interaction.

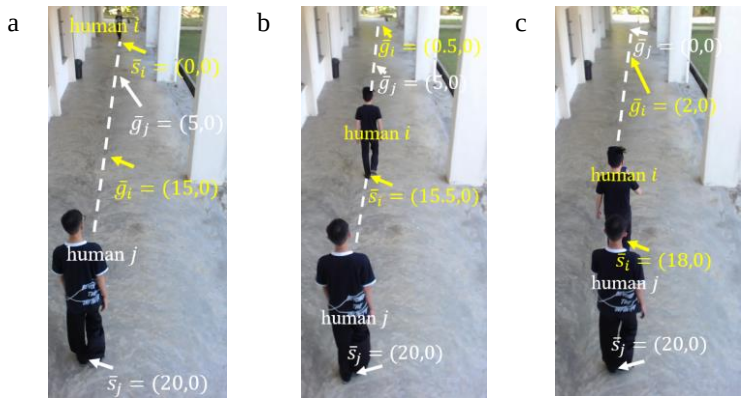

Fig. 6 - (a) Scenario 1 (S1); (b) Scenario 2 (S2) (c); Scenario 3 (S3).

Three human scenarios (Fig. 6) were used to collect the human state data. These scenarios are scenarios used by previous literatures. Scenario 1 (S1): face-to-face encounter [9, 12, 13, 21, 23, 24] (Fig. 6a), Scenario 2 (S2): walking-away [19] (Fig. 6b), Scenario 3 (S3): overtaking (Fig. 6c) [12]. A total of 16 human subjects were involved, only male subjects with age between 19 to 24 years old (young adult group [25]) were chosen to remove the dependence of the training data on demographic factors (gender and age). The subjects were randomly split into 2 groups, one representing human i while the other represents human j. Each subject from the groups were then randomly assigned a label from 1 to 8. The data collection started with S1 where subjects with label 1 from each group were positioned at $\bar{s}_i$ and $\bar{s}_j$ respectively. The subjects were instructed to walk towards their respective goal $\bar{g}_i$ and $\bar{g}_j$ and their movements were recorded. This was repeated for 3 times before changing the subjects to the consecutive labels. Data collection for S1 was completed when all subjects from label 1 to 8 were involved, and the same procedures were repeated for S2 and S3.

The human state data were then collected by tracking the human in the video footage using Kernelized Correlation Filters (KCF) [26] in OpenCV. The neural-network model was then trained using Levenberg-Marquardt backpropagation algorithm [27]. The output of the trained model, f_{NN} is then used to adaptively scale the size of the personal-space when different human states are encountered.

The f_{NN} effect on the size of the personal-space towards different human states are shown in Fig. 7. When human n was moving towards robot q (Fig. 7a), the size of the personal-space increased. Fig. 7b to Fig. 7d show the scenario where human n was facing away from robot q. As shown in Fig. 7b, when human n was much faster than robot q ($\tilde{v}_{nq} = 0.0$), the size of the personal-space remained small regardless of their relative distance. Fig. 7c shows that, when human n was walking slightly slower than robot q ($0.0 < \tilde{v}_{nq} < 0.5$), the size of the personal-space decreased as their relative distance decreased. Fig. 7d shows that, when human n was walking much slower than robot q ($\tilde{v}_{nq} > 0.5$), the size of the personal-space decreased as their relative distance decreased, but the size was larger than that in the previous case

($0.0 < \tilde{v}_{nq} < 0.5$). These changes in the size of personal-space allow a robot to adapt to different human states and prioritize avoiding certain human over the other to improve navigation performance.

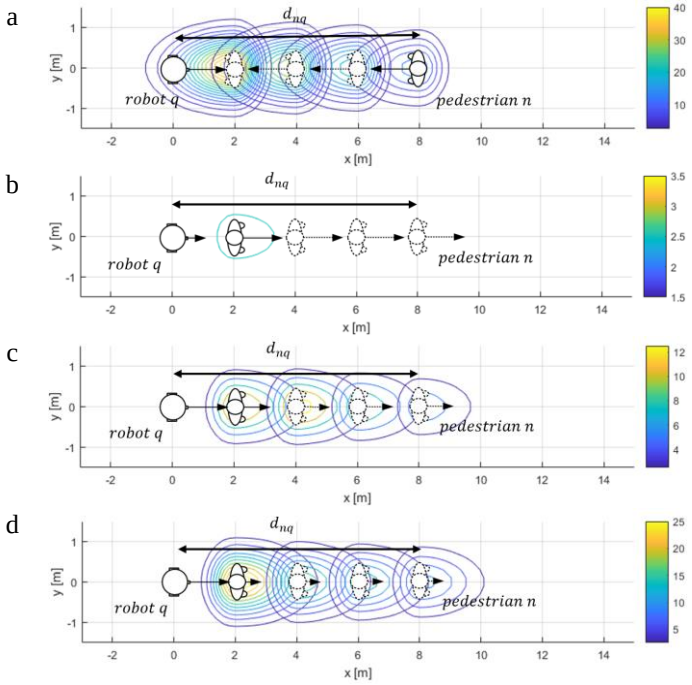

Fig. 7 - (a) $\omega(\varphi_{nq}) \geq 0.5$ at varying $\tilde{d}_{nq}$; (b) $\omega(\varphi_{nq}) \leq 0.5$ at $\tilde{v}_{nq} = 0.0$ and varying $\tilde{d}_{nq}$; (c) $\omega(\varphi_{nq}) \leq 0.5$ at $0.0 < \tilde{v}_{nq} < 0.5$ and varying $\tilde{d}_{nq}$; (d) $\omega(\varphi_{nq}) \leq 0.5$ at $\tilde{v}_{nq} > 0.5$ and varying $\tilde{d}_{nq}$.

To evaluate whether the proposed NNPC can improve the navigation performance, several human-robot scenarios were involved. The evaluation was carried out in a human-robot simulator [28] using manufacturing scenarios and were designed by benchmarking several human-aware navigation literatures [12, 13, 19, 23]. The scenarios were also setup to include a robot encountering human at different states, to test whether NNPC can adapt to changes in states. The first to forth scenarios involve robot encountering a human worker in a factory with several production lines as obstacles. The first scenario (SS1) as shown in Fig. 8a was a face-to-face human-robot encounter. Fig. 8b, the second scenario (SS2) involved a human walking parallel to and eventually away from the robot. The robot behaviour in SS1 and SS2 were used for evaluating NNPC towards the change in human angular position. Scenario 3 (SS3) was setup similar to SS2, but with a decreased in human velocity from 1.4 ms^{-1} [29] to 0.25 ms^{-1} and the human initial and goal positions were setup as (0,1) and (7,1) respectively. The robot behaviors in SS2 and SS3 were used to evaluate whether NNPC can adapt to changes in human velocity. The forth scenario was designed similar to SS3, but with an increased in the initial human-robot distance where the human initial and goal positions were setup as (7,1) and (12,1) respectively. The robot behaviors in SS3 and SS4 were utilized to test whether NNPC can adapt to human at different linear positions.

a

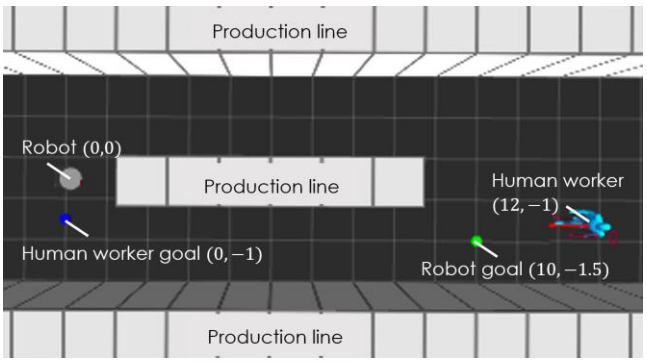

b

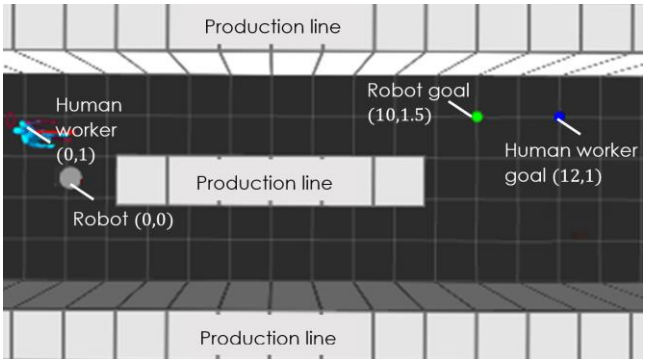

Fig. 8 - (a) face-to-face human-robot encounter; (b) human facing away from robot encounter.

The fifth scenario (SS5) as shown in Fig. 9 was used to test whether NNPC can handle higher human density scenario where a robot can possibly encounter in real life, for example, groups of workers exiting a factory through a pathway during recess time. The performance of NNPC was compared against two prior mentioned human-aware costmap methods: proxPL (Equation 7) by Kirby et al. [7] and proxHIPL (Equation 8), a combination of methods by Kirby et al. [7] and Karageorgas [13]. The performance metrics used were based on three criteria: human safety and comfort, path smoothness and navigation efficiency. The criteria and their respective metrics are shown in Table 1.

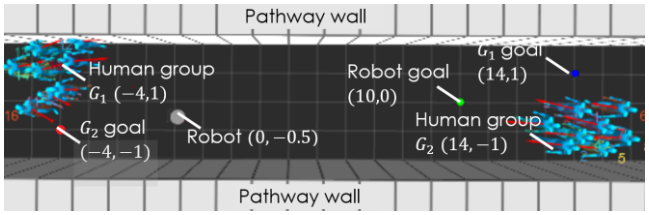

Fig. 9 - robot encounters human worker groups.

Table 1 - Performance criteria and their respective metrics.

Criteria	Metrics	Symbol
Human safety and comfort	Minimum relative human-robot distance	$d_{rel_{min}}$
Path smoothness	Average integral of linear jerk	$I_{j_{lin}}$
	Average integral of angular jerk	$I_{j_{ang}}$
Navigation efficiency	Execution time	t_{task}
	Path length	L_p

4. Results and Discussion

a b

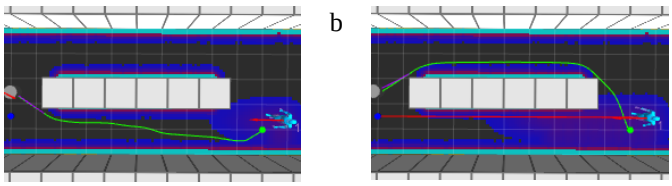

Fig. 10 - robot behaviours in SS1 using (a) proxPL; (b) proxHIPL/ NNPC.

Fig. 10a shows that, for SS1, proxPL was unable to predict human future trajectories which ended up choosing the bottom lane and moved too close to the human ($d_{rel_{min}} = 0.79\ m$), which can cause human safety issues. NNPC with human path prediction was able to perform as well as proxHIPL by choosing the top lane, avoided getting too near to the

human with $d_{rel_{min}}$ value of 1.97 m and 2.08 m respectively. For path smoothness, in terms of $I_{j_{lin}}$, NNPC (1.25 ms^{-3}) was significantly better ($p > 0.05$) than proxPL (1.43 ms^{-3}) because the robot with proxPL had to come to an emergency stop when the human suddenly appeared around the corner of the bottom lane. NNPC had no significant difference ($p > 0.05$) in terms of $I_{j_{ang}}$ as compared to other methods. NNPC and proxHIPL had greater execution time and path length as compared to proxPL because the top lane was chosen to provide better human safety and comfort.

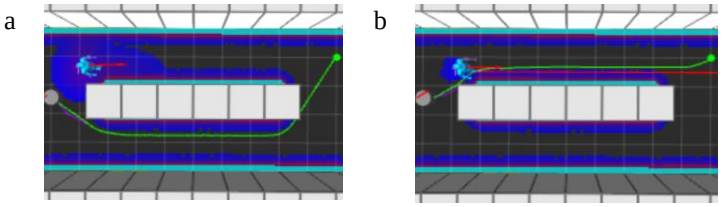

Fig. 11 - robot behaviours in SS2 using (a) proxPL/ proxHIPL; (b) NNPC.

For SS2, Fig. 11a shows the robot behaviour of proxPL where the robot chose the longer path because the large size of the generated human personal-space was blocking the top lane. The non-adaptive proxHIPL also had the similar issue as shown in Fig. 11a. NNPC however managed to adapt to the human angular position, generated a smaller sized personal-space which allowed the robot to plan a shorter path through the top lane (Fig. 11b). $d_{rel_{min}}$ is not used in SS2, SS3 and SS4 as all costmaps would have the similar values which equate to either the initial or final human-robot distance. In terms of $I_{j_{lin}}$, NNPC (0.96 ms^{-3}) had an improvement of 9.44 % as compared to proxPL (1.06 ms^{-3}) and 12.32 % as compared to proxHIPL (1.09 ms^{-3}). In terms of $I_{j_{ang}}$, NNPC (10.03 ms^{-3}) had a significant improvement ($p \leq 0.001$) of 20.96 % as compared to proxPL (12.69 ms^{-3}) and 19.40 % as compared to proxHIPL (12.44 ms^{-3}). For navigation efficiency, NNPC had significant improvements in both t_{task} and L_p. For t_{task}, NNPC (22.22 s) had an improvement of 16.62 % and 16.87 % as compared to proxPL (26.65 s) and proxHIPL (26.73 s) respectively. For L_P, NNPC (10.66 m) had an improvement of 12.26 % as compared to both proxPL and proxHIPL (12.15 m). These improvements show that the by adapting to human angular position, the navigation performance can be improved.

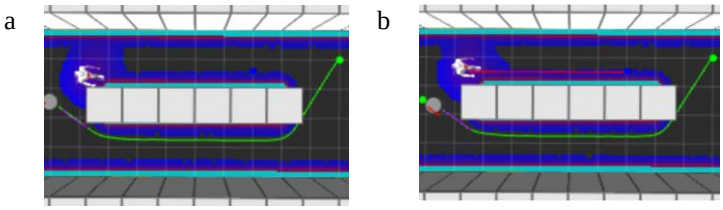

Fig. 12 - robot behaviours in SS3 using (a) proxPL; (b) proxHIPL/ NNPC.

For SS3 where the human encountered was walking slowly, the personal-space generated by proxPL (Fig. 12a), proxHIPL and NNPC in Fig. 12b generated similar sized personal-space. This shows that NNPC was able to adapt to the slow-moving human and generate a larger sized personal-space as compared to the one in SS2 (Fig. 10b). This allowed the robot to select a faster path when the slow-moving human was blocking the top lane and at the same time avoid getting too close to the human for safety and comfort purposes. NNPC performed as well as proxPL and proxHIPL in SS3 where the performance metrics (Table 2) of NNPC show no significant difference ($p > 0.05$) as compared the other approaches.

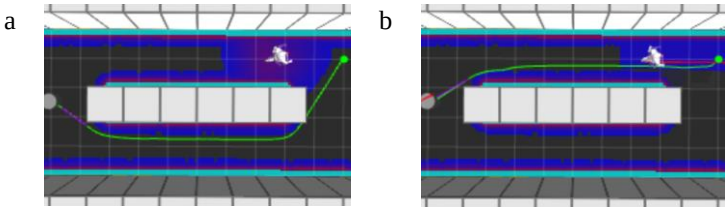

Fig. 13 - robot behaviours in SS4 using (a) proxPL/ proxHIPL; (b) NNPC.

For SS4, Fig. 13a shows the costmap generated by proxPL blocked the top lane and caused the robot to take a longer path. The non-adaptive proxHIPL also faced the similar problem as shown in Fig. 13a. NNPC however adapted to the change in human linear position, generated a smaller sized personal-space, allowing the robot to plan a shorter path

towards the goal. NNPC significantly outperformed ($p \leq 0.001$) proxPL and proxHIPL in all metrics. In terms of $I_{j_{lin}}$, NNPC ($0.82\ ms^{-3}$) was 23.36 % and 18.00 % lower than proxPL ($1.07\ ms^{-3}$) and proxHIPL ($1.00\ ms^{-3}$) respectively. For $I_{j_{ang}}$, NNPC ($9.85\ rads^{-3}$) had improvements of 25.72 % and 24.58 % as compared to proxPL ($13.26\ rads^{-3}$) and proxHIPL ($13.06\ rads^{-3}$) respectively. For navigation efficiency, in terms of t_{task}, NNPC ($22.10\ s$) improved by 17.01 % as compared to proxPL ($26.63\ s$) and 17.44 % as compared to proxHIPL ($26.77\ s$). NNPC ($10.63\ m$) also had shorter L_p, 12.51 % shorter than proxPL ($12.15\ m$) and 12.73 % shorter than proxHIPL ($12.18\ m$). These improvements show that the adaptive behaviour of NNPC towards human linear position can improve the path smoothness and navigation efficiency.

a b

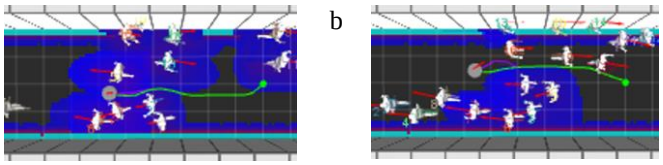

Fig. 14 - robot behaviours in SS5 using (a) proxPL/ proxHIPL; (b) NNPC.

In a higher human density scenario (SS5), Fig. 14a shows that proxPL overpopulated the costmap with human personal-space, where the robot wrongly avoided the G_1 which was initially closer to the robot. This caused the robot to detour towards the wrong side and moved too close to G_2. The non-adaptive proxHIPL also had similar behaviour as shown in Fig. 14a. NNPC however, was able to reduce the size of the personal-space for G_1 that was moving towards the same direction as the robot, but not the oncoming G_2. This helped the robot to prioritized in avoiding the oncoming group and joined the other group to navigate towards the goal. For human safety and comfort ($d_{rel_{min}}$), NNPC ($0.68\ m$) outperformed proxPL ($0.38\ m$) by 78.95 % and proxHIPL ($0.47\ m$) by 44.68 %. For $I_{j_{lin}}$, NNPC ($1.79\ ms^{-3}$) had significant improvement ($p \leq 0.001$), where it was 36.07 % better than proxPL ($2.80\ ms^{-3}$) and 37.63 % better than proxHIPL ($2.87\ ms^{-3}$). In terms of t_{task}, NNPC ($22.72\ s$) also significantly improved ($p \leq 0.001$) by 21.03 % as compared to proxPL ($28.77\ s$) and 24.84 % as compared to proxHIPL ($30.23\ s$). In terms of $I_{j_{ang}}$ and L_p, NNPC had no significant difference as compared to other methods as all methods caused the robot to make certain detours, that increased angular jerk and path length, but the robot with NNPC detoured to the correct side while the robot with proxPL and proxHIPL detoured to the wrong side. These improvements show that the adaptive capability of NNPC improved the navigation performance in a multiple human scenario. Table 2 shows the navigation performance for each costmap in all human scenarios, with highlighted improvements made by NNPC.

Table 1 – Navigation performance

Scenario	Costmap	$d_{rel_{min}}$ $[m]$	$I_{j_{lin}}$ $[ms^{-}$	$I_{j_{ang}}$ $[rads^{-}$	t_{task} $[s]$	L_p $[m]$
SS1	proxPL	0.79	1.43	10.59	24.27	10.60
	proxHIPL	2.08	1.36	9.90	26.12	12.10
	NNPC	2.03	1.25	10.59	25.67	12.21
SS2	proxPL	–	1.06	12.69	26.65	12.15
	proxHIPL	–	1.09	12.44	26.73	12.15
	NNPC	–	0.96	10.03	22.22	10.66
SS3	proxPL	–	1.17	12.87	26.26	12.17
	proxHIPL	–	1.15	13.31	26.20	12.14
	NNPC	–	1.16	12.89	26.25	12.20
SS4	proxPL	–	1.07	13.26	26.63	12.15
	proxHIPL	–	1.00	13.06	26.77	12.18
	NNPC	–	0.82	9.85	22.10	10.63
SS5	proxPL	0.38	2.80	14.60	28.77	10.52
	proxHIPL	0.47	2.87	13.32	30.23	10.78
	NNPC	0.68	1.79	14.53	22.72	10.80

5. Conclusion

In this study, a neural-network based adaptive proxemic costmap, named NNPC is introduced to overcome the drawbacks of current human-aware costmap methods. The neural-network proxemic model of NNPC was trained using human state data from real human subjects. NNPC then used the model output to generate different sized personal-space based on various human state encounters. By adapting to the changing human states, NNPC managed to significantly outperform two other costmap methods in both single and multiple human scenarios, in terms of human safety and comfort, path smoothness and navigation efficiency. Future works can take account of human demographic and social relationship as model input to further improve the human-aware navigation performance.

Acknowledgement

The authors are grateful to Universiti Teknologi Malaysia for providing facilities to conduct this research and this work is supported by the Universiti Teknologi Malaysia Research Grant (04G42 and 16H47). Besides, the authors also thank to DF Automation & Robotics Sdn Bhd for supplying the test robotic platform.

References

[1] Bahrin, M. A. K., Othman, M. F., Azli, N. N. and Talib, M. F. (2016). Industry 4.0: A review on industrial automation and robotic. JURNAL TEKNOLOGI, 78(6-13),137-143.
[2] Hall, E. T. (1990). The Hidden Dimension. 27th ed. Anchor Books.
[3] Chik, S. F., Yeong, C. F., Su, E. L. M., Lim, T. Y., Subramaniam, Y. and Chin, P. J. H. (2016). A Review of Social-Aware Navigation Frameworks for Service Robot in Dynamic Human Environments. Journal of Telecommunication, Electronic and Computer Engineering (JTEC). 8(11), 41-50.
[4] Papadakis, P., Spalanzani, A. and Laugier, C. (2013). Social mapping of human-populated environments by implicit function learning. Proceedings of the 2013 IEEE/RSJ International Conference on Intelligent Robots and Systems. Tokyo Big Sight, Tokyo, 1701-1706.
[5] Gómez, J. V., Mavridis, N. and Garrido, S. (2013). Social path planning: Generic human-robot interaction framework for robotic navigation tasks. Proceedings of the 2nd Intl. Workshop on Cognitive Robotics Systems: Replicating Human Actions and Activities. Tokyo, Japan.
[6] Vega-Magro, A., Manso, L., Bustos, P., Núñez, P. and Macharet, D. G. (2017). Socially acceptable robot navigation over groups of people. Proceedings of the 2017 26th IEEE International Symposium on Robot and Human Interactive Communication (RO-MAN). Lisbon, Portugal, 1182-1187.
[7] Kirby, R., Simmons, R. and Forlizzi, J. (2009). COMPANION: A Constraint-Optimizing Method for Person-Acceptable Navigation. Proceedings of the 18th IEEE International Symposium on Robot and Human Interactive Communication (RO-MAN 2009). Toyama International Conference Center, Japan, 607-612.
[8] Bitgood, S. and Dukes, S. (2006). Not Another Step! Economy of Movement and Pedestrian Choice Point Behavior in Shopping Malls. Environment and Behavior. 38(3), 394-405.
[9] Scandolo, L. and Fraichard, T. (2011). An anthropomorphic navigation scheme for dynamic scenarios. Proceedings of the 2011 IEEE International Conference on Robotics and Automation (ICRA). Shanghai International Conference Center, Shanghai, China, 809-814.
[10] Patompak, P., Jeong, S., Chong, N. Y. and Nilkhamhang, I. (2016). Mobile robot navigation for human-robot social interaction. Proceedings of the 2016 16th International Conference on Control, Automation and Systems (ICCAS). HICO, Gyeongju, Korea, 1298-1303.
[11] Helbing, D. and Molnar, P. (1995). Social force model for pedestrian dynamics. Physical review E. 51(5), 4282.
[12] Kollmitz, M., Hsiao, K., Gaa, J. and Burgard, W. (2015). Time dependent planning on a layered social cost map for human-aware robot navigation. Proceedings of the 2015 European Conference on Mobile Robots (ECMR). Lincoln, UK, 1-6.
[13] Karageorgos, D. (2017). Human-Aware Autonomous Navigation of a Care Robot in Domestic Environments. Masters Thesis. Delft University of Technology.
[14] Ferrer, G. and Sanfeliu, A. (2014). Bayesian Human Motion Intentionality Prediction in urban environments. Pattern Recognition Letters. 44,134-140.
[15] Rabiner, L. R. (1989). A tutorial on hidden Markov models and selected applications in speech recognition. Proceedings of the IEEE. 77(2), 257-286.
[16] Hart, P. E., Nilsson, N. J. and Raphael, B. (1968). A Formal Basis for the Heuristic Determination of Minimum Cost Paths. IEEE Transactions on Systems Science and Cybernetics. 4(2), 100-107.
[17] Johansson, A., Helbing, D. and Shukla, P. K. (2007). Specification of the social force pedestrian model by evolutionary adjustment to video tracking data. Advances in complex systems. 10(supp02), 271-288.
[18] Al Shalabi, L., Shaaban, Z. and Kasasbeh, B. (2006). Data mining: A preprocessing engine. Journal of Computer Science. 2(9), 735-739.
[19] Kim, B. and Pineau, J. (2016). Socially Adaptive Path Planning in Human Environments Using Inverse Reinforcement Learning. International Journal of Social Robotics. 8(1), 51-66.

[20] Vasquez, D., Okal, B. and Arras, K. O. (2014). Inverse reinforcement learning algorithms and features for robot navigation in crowds: an experimental comparison. Proceedings of the 2014 IEEE/RSJ International Conference on Intelligent Robots and Systems (IROS). Chicago, Illinois, US, 1341-1346.
[21] Ratsamee, P., Mae, Y., Kamiyama, K., Horade, M., Kojima, M. and Arai, T. (2015). Social interactive robot navigation based on human intention analysis from face orientation and human path prediction. ROBOMECH Journal. 2(1), 11.
[22] Kretzschmar, H., Spies, M., Sprunk, C. and Burgard, W. (2016). Socially compliant mobile robot navigation via inverse reinforcement learning. The International Journal of Robotics Research. 35(11), 1289-1307.
[23] Lu, D. V. and Smart, W. D. (2013). Towards more efficient navigation for robots and humans. Proceedings of the 2013 IEEE/RSJ International Conference on Intelligent Robots and Systems. Tokyo Big Sight, Tokyo, 1707-1713.
[24] Nishitani, I., Matsumura, T., Ozawa, M., Yorozu, A. and Takahashi, M. (2015). Human-centered X-Y-T space path planning for mobile robot in dynamic environments. Robotics and Autonomous Systems. 66, 18-26.
[25] Geifman, N. and Rubin, E. (2012). The Age-Phenome Knowledgebase: an example to handling abstraction and expressiveness in a knowledge domain. Proceedings of the Conference: Conference: Conference on Semantics in Healthcare and Life Sciences (CSHALS). Cambridge, Massachusetts, United States.
[26] Henriques, J. F., Caseiro, R., Martins, P. and Batista, J. (2015). High-Speed Tracking with Kernelized Correlation Filters. IEEE Transactions on Pattern Analysis and Machine Intelligence. 37(3), 583-596.
[27] Hagan, M. T. and Menhaj, M. B. (1994). Training feedforward networks with the Marquardt algorithm. IEEE Transactions on Neural Networks. 5(6), 989-993.
[28] Okal, B. and Arras, K. O. (2014). Towards Group-Level Social Activity Recognition for Mobile Robots. Proceedings of the 2014 IEEE/RSJ International Conference on Intelligent Robots and Systems (IROS). Chicago, Illinois, US.
[29] Barton, H., Grant, M. and Guise, R. (2003). Shaping neighbourhoods: a guide for health, sustainability and vitality. Taylor & Francis